REFERENCES AND NOTES

1. K. S. Suslick, Ed., *Ultrasound: Its Chemical, Physical, and Biological Effects* (VCH Publishers, New York, 1988).
2. K. S. Suslick, *Sci. Am.* **260**, 80 (February 1989).
3. ———, *Adv. Organomet. Chem.* **25**, 73 (1986).
4. ——— and E. B. Flint, *Nature* **330**, 553 (1987); E. B. Flint and K. S. Suslick, *J. Am. Chem. Soc.* **111**, 6987 (1989).
5. K. S. Suslick, R. E. Cline, Jr., D. A. Hammerton, *J. Am. Chem. Soc.* **108**, 5641 (1986).
6. K. S. Suslick and D. J. Casadonte, *ibid.* **109**, 3459 (1987).
7. K. S. Suslick, *Mod. Syn. Methods* **4**, 1 (1986).
8. C. Einhorn *et al.*, *Synthesis* **11**, 787 (1989).
9. J. Lindley and T. J. Mason, *Chem. Soc. Rev.* **16**, 275 (1987).
10. K. S. Suslick, D. J. Casadonte, S. J. Doktycz, *Solid State Ionics* **32/33**, 444 (1989).
11. ———, *Chem. Materials* **1**, 6 (1989).
12. K. S. Suslick and S. J. Doktycz, *Adv. Sonochem.*, in press.
13. ———, *J. Am. Chem. Soc.* **111**, 2342 (1989).
14. J. C. de Souza-Baroza, C. Petrier, J. L. Luche, *J. Org. Chem.* **53**, 1212 (1988).
15. J. Lindley, T. J. Mason, J. P. Lorimer, *Ultrasonics* **25**, 45 (1987).
16. W. Lauterborn and W. Hentschel, *ibid.* **24**, 59 (1985).
17. ———, *ibid.* **25**, 260 (1986).
18. C. M. Preece and I. L. Hansson, *Adv. Mech. Phys. Surf.* **1**, 199 (1981).
19. E. A. Neppiras, *Phys. Rep.* **61**, 159 (1980).
20. R. C. Weast, Ed., *CRC Handbook of Chemistry and Physics* (CRC Press, Boca Raton, FL, 1989), p. D-43.
21. R. H. Cole, *Underwater Explosions* (Princeton Univ. Press, Princeton, NJ, 1948).
22. A. Vogel and W. Lauterborn, *J. Acoust. Soc. Am.* **84**, 719 (1988).
24. We appreciate the use of the Center for Microanalysis of Materials, University of Illinois at Urbana-Champaign, supported by the U.S. Department of Energy under contract DE-AC-02-76ER-01198. Support of the NSF is greatly appreciated. K.S.S. gratefully acknowledges an NIH Research Career Development Award.

24 August 1989; accepted 13 December 1989

Gaussian Free-Energy Dependence of Electron-Transfer Rates in Iridium Complexes

LUCIUS S. FOX, MARIUSZ KOZIK, JAY R. WINKLER, HARRY B. GRAY

The kinetics of photoinduced electron-transfer (ET) reactions have been measured in a series of synthetic donor-acceptor complexes. The electron donors are singlet or triplet excited iridium(I) dimers (Ir_2), and the acceptors are *N*-alkylpyridinium groups covalently bound to phosphinite ligands on the Ir_2 core. Rate constants for excited-state ET range from 3.5×10^6 to 1.1×10^{11} per second, and thermal back ET (pyridinium radical to Ir_2^+) rates vary from 2.0×10^{10} to 6.7×10^7 per second. The variation of these rates with driving force is in remarkably good agreement with the Marcus theory prediction of a Gaussian free-energy dependence.

THE PRIMARY CHARGE SEPARATION in the bacterial photosynthetic reaction center proceeds in less than 5 ps and is virtually independent of temperature (*1*). Subsequent ET steps that increase the charge-separation distance, and ultimately lead to photochemical energy storage, are all faster than energy-wasting charge-recombination events (*2*). If we are to prepare synthetic systems that emulate natural photosynthesis, thorough comprehension of all factors governing ET rates is essential. In semiclassical ET theory, three parameters govern the reaction rates: (i) the electronic coupling between the donor and acceptor (κ_E), (ii) the free-energy change for the reaction ($\Delta G°$), and (iii) a parameter (λ) related to the extent of inner-shell and solvent nuclear reorganization accompanying the ET reaction (*3*). Moreover, when intrinsic ET barriers are small, the dynamics of nuclear motion can limit ET rates through the frequency factor ν_N. These parameters describe the rate of ET between a donor and acceptor held at a fixed distance and orientation (Eq. 1),

$$k_{ET} = \nu_N \kappa_E \exp\left[\frac{-(\Delta G° + \lambda)^2}{4\lambda RT}\right] \qquad (1)$$

where R is the gas constant and T is the absolute temperature.

The surprising prediction of a Gaussian free-energy dependence for k_{ET} has stimulated numerous experimental investigations (*4–11*). Early attempts to verify Eq. 1 were frustrated by diffusion-limited rates at high driving forces in bimolecular ET reactions. Our previous examination of the ET quenching of the triplet excited state of $[Ir_2(\mu\text{-pz})_2(COD)_2]$ (pz = pyrazolyl; COD = 1,5-cyclooctadiene) by alkylpyridinium acceptors is a case in point (*6*). At driving forces between 0.1 and 0.8 eV, the quenching rate constant increases monotonically. At higher driving forces, the rates plateau at $10^{10} M^{-1}$ s^{-1}. No evidence was found for a decrease in ET rate at driving forces up to 1.18 eV.

In order to circumvent the bimolecular diffusion limit, we have prepared a set of complexes in which the electron donor and acceptor are covalently coupled into one molecule, $[Ir_2(\mu\text{-pz}^*)_2(CO)_2(Ph_2PO(CH_2)_2A^+)_2]$ (pz* = 3,5-dimethylpyrazolyl; Ph = C_6H_5). The Ir(I) dimer (Ir_2) serves as the electron donor, and the acceptors (A^+) are *N*-alkylpyridinium groups bound to phosphinite ligands (Fig. 1). An x-ray crystal structure determination of the complex with A^+ = pyridinium (py^+) reveals a 5.8 Å separation between the closer Ir center and the N atom of the pyridinium ring (*12*). In its lowest singlet (^1B) and triplet (^3B) excited states, the Ir_2 chromophore is a potent reductant that is capable of transferring an electron to a covalently attached pyridinium cation (*12, 13*).

We reported previously that ET quenching of the ^1B excited state in two of the donor-acceptor complexes (A^+ = pyridin-

Table 1. Photophysical parameters for Ir_2-phosphinite complexes (Me, methyl; Et, ethyl). Quantum yields (ϕ_f, singlet quantum yield; ϕ_p, triplet quantum yield) taken from spectra measured in acetonitrile solutions at room temperature with $Ru(2,2'\text{-bipyridine})_3^{2+}$ used as a standard; excitation wavelength = 436 nm (*25*). Singlet quantum yields for the reference complexes are ±10%; triplet quantum yields are ±30%. Singlet quantum yields for the donor-acceptor complexes are ±30%; triplet quantum yields are ±80%. Singlet lifetime is τ_f; triplet lifetime is τ_p.

Phosphinite	ϕ_f	ϕ_p	τ_f (ps)	τ_p† (μs)
Reference complexes				
$Ph_2POCH_2CH_2\text{-}NEt_3^+$	0.0015	0.032	95*	1.2
$Ph_2POCH_2CH_3$	0.0023	0.025	100*	1.1
Ph_2POCH_3	0.0027	0.040	100‡	1.2
$Ph_2PO(CH_2)_3CH_3$	0.0025	0.030	100‡	1.1
Donor-acceptor complexes				
$Ph_2POCH_2CH_2Me_3py^+$	0.00017	0.0013	25†	0.012 0.144
$Ph_2POCH_2CH_2\text{-}4\text{-}Mepy^+$	0.00006	0.0004	9†	0.003
$Ph_2POCH_2CH_2\text{-}py^+$	0.00003	§	4.4‖	§

*Determined from transient absorption measurements; ±20%. †Determined from time-resolved emission measurements; ±10%. ‡Estimated from quantum yields and the singlet lifetime of $[Ir_2(pz^*)_2(CO)_2(Ph_2POCH_2CH_3)_2]$; ±10%. §Emission too weak to measure. ‖Estimated from quantum yields and singlet lifetime of $[Ir_2(pz^*)_2(CO)_2(Ph_2POCH_2CH_3)_2]$; ±30%.

L. S. Fox and H. B. Gray, Arthur Amos Noyes Laboratory, California Institute of Technology, Pasadena, CA 91125.
M. Kozik and J. R. Winkler, Department of Chemistry, Brookhaven National Laboratory, Upton, NY 11973.

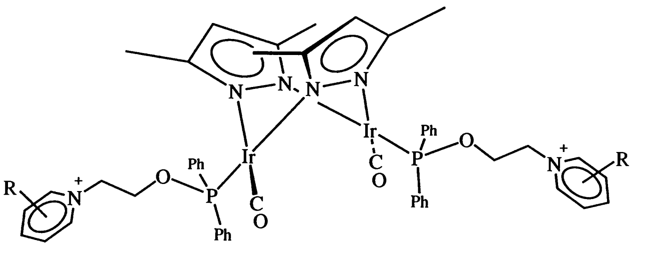

Fig. 1. The ET driving force varies with the substituent R in the Ir_2-A^+ complexes.

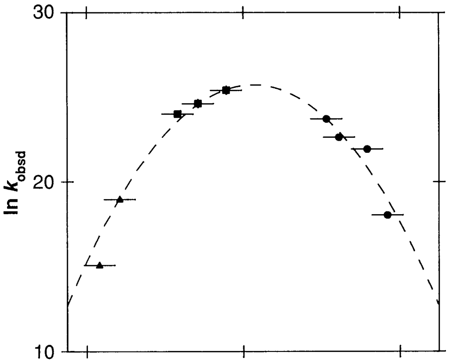

Fig. 2. Plot of ln k versus driving force ($-\Delta G°$) for reactions of Ir_2-A^+ in acetonitrile solution at room temperature (Table 2): ^{1}ET (■); ^{3}ET (▲); and ET^b (●). The dashed line is the best fit of these data to Eq. 1.

ium and 4-phenylpyridinium) takes place on a picosecond time scale ($k_{ET} \geqq 10^{11}$ s^{-1}) (*13*). The rates of hole:electron recombination in these reactions proved to be 1/5 to 1/10 as fast as the excited-state ET reactions. We have now completed an investigation of the kinetics of Ir_2-A^+ ET reactions in acetonitrile solution in which the driving forces span a range of 0.08 to 1.92 eV. The reactions include photoinduced ET from the singlet ($^1Ir_2$* to py^+:^{1}ET) and triplet ($^3Ir_2$* to py^+:^{3}ET) excited states of Ir_2, as well as thermal back ET ($py^•$ to Ir_2^+:ET^b). The point of these studies was to test the free-energy dependence predicted by Eq. 1 and to determine what differences, if any, could be found among these three types of ET processes.

The rates of ^{1}ET, ^{3}ET, and ET^b reactions in the series of Ir_2 complexes were evaluated from a combination of time-resolved and steady-state absorption and luminescence spectroscopies (*14*). The photophysical parameters measured for these molecules are summarized in Table 1. All ^{1}ET and ^{3}ET rates have been multiplied by a factor of 0.5 to account for the 1:2 donor:acceptor stoichiometry in these complexes. The ET rate constants and driving forces are given in Table 2 (*12*). The rates of excited-state ET increase with driving force and maximize at 1.1×10^{11} s^{-1} near $-\Delta G° = 1$ eV. The ET^b rates, however, decrease by two orders of magnitude as $-\Delta G°$ increases from 1.5 to 1.9 eV. This "inverted" free-energy behavior is predicted by Eq. 1 for driving forces greater than λ.

The best fit of the driving-force data to Eq. 1 appears as a dashed line in Fig. 2. Optimum values for the two adjustable parameters are $\nu_N\kappa_E = 1.5 \times 10^{11}$ s^{-1} and $\lambda = 1.06$ eV (*15*). The maximum ET rate for the system, $\nu_N\kappa_E$, is proportional to the square of the matrix element, H_{AB}, that describes the electronic coupling between donor and acceptor sites. Evaluation of H_{AB} in the nonadiabatic limit (*3*) yields a value of 24 cm^{-1} for the Ir_2 complexes (*15*). This value agrees well with that found for a porphyrin-quinone complex in which the edge-to-edge donor-acceptor separation is 5.5 Å ($H_{AB} = 30$ cm^{-1}) (*7*) and, interestingly, with that estimated for the bacterial photosynthetic reaction center ($H_{AB} = 25$ cm^{-1}) (*16*).

The reorganization parameter λ in Eq. 1 arises from a classical description of the nuclear reorientation associated with the ET reaction (*3*). Both inner-sphere (λ_{IN}) and solvent (λ_{OUT}) motions contribute to this reorganization. Distortions of the Ir_2 core upon excitation to ^1B and ^3B states, or upon one-electron oxidation, are likely to involve primarily the Ir-Ir separation. Metal-metal compressions of about 0.2 to 0.3 Å have been reported for excited Rh(I) and Pt(II) dimers, and analyses of the absorption and emission profiles indicate $\lambda \leqq 0.2$ eV for the excitation process (*17*). On the basis of crystal structure analyses of closely related complexes (*18*), we estimate that oxidation of Ir_2 to Ir_2^+ would reduce the Ir-Ir separation by roughly 0.1 Å, contributing 0.05 to 0.1 eV to λ_{IN}. A small addition to λ_{IN} also arises from expansion of the py ring upon radical formation. All of these distortions are relatively minor, however, and the overall λ_{IN} contribution to λ is not likely to be more than 0.2 eV. Reorganization of the polar solvent (CH_3CN) should furnish the major component of λ in these ET reactions. Dielectric continuum models are generally used to estimate the magnitude of λ_{OUT} (*19*). Representing the Ir_2 donor-acceptor complex as a sphere (19.14 Å in diameter) of low dielectric constant ($\epsilon_0 = 3$) embedded in a continuous dielectric ($\epsilon_0 = 36$) leads to an estimate of $\lambda_{OUT} = 0.8$ eV (*20*). The experimental reorganization energy is clearly in good agreement with the predictions of ET theories. It is interesting to note that $\lambda = 1.06$ eV is nearly the same as the value found in bimolecular $^3Ir_2$*/py^+-R quenching (*6*).

An implicit assumption of the preceding analysis is that H_{AB}, λ_{OUT}, and λ_{IN} are constant for all ^{1}ET, ^{3}ET, and ET^b reactions that we have examined. Wave functions for singlet states, triplet states, and radicals, however, are known to vary substantially in spatial extent and polarizability (*21*). Furthermore, theoretical studies of the electronic coupling matrix element (*22*) and the outer-sphere reorganization energy (*23*) have suggested that both parameters might vary with reaction type. The remarkably close agreement between the experimental results and the semiclassical ET theory described by Eq. 1 implies, however, that in the Ir_2 system the variations in H_{AB} and λ are not great (*24*).

The most striking feature of the Ir_2 ET kinetics is the strongly inverted free-energy dependence at high driving forces. In the semiclassical ET theory, inverted driving-force effects arise from a reduction in the Franck-Condon factor for ET as $-\Delta G°$ increases beyond the value of λ (*3*).

Table 2. Driving forces and rate constants for ET. Standard errors are 0.1 eV for $-\Delta G°$ and ±10% for k_{ET}, except where noted.

Donor	Acceptor	$-\Delta G°$ (eV)	k_{ET} (s^{-1})
$^3Ir_2$*	2,4,6-Me_3py^+	0.08	3.5×10^6
$^3Ir_2$*	4-$Mepy^+$	0.21	1.7×10^8
$^1Ir_2$*	2,4,6-Me_3py^+	0.58	2.7×10^{10}
$^1Ir_2$*	4-$Mepy^+$	0.71	5.0×10^{10}*
$^1Ir_2$*	py^+	0.89	1.1×10^{11}
$^1Ir_2$*	4-$Phpy^+$	0.97	$>1.1 \times 10^{11}$
4-$Phpy^•$	Ir_2^+	1.53	2.0×10^{10}
4-$Mepy^•$	Ir_2^+	1.61	6.7×10^9
$py^•$	Ir_2^+	1.79	3.3×10^9
2,4,6-$Me_3py^•$	Ir_2^+	1.92	6.7×10^7

*±30%.

The Ir_2 complex with $A^+ = 2,4,6\text{-}Me_3py^+$ (Me = methyl) provides a clear example of this effect (Table 2). The ^1ET rate in this molecule is more than 300 times the ET^b rate, although the latter process has a 1.3 eV greater driving force. Maximizing both the ^1ET rate and the $^1ET/ET^b$ ratio are the primary requirements for the efficient generation and maintenance of photoinduced hole:electron separation. The Ir_2 ET data clearly demonstrate that the driving force–dependent Franck-Condon barrier to ET can be exploited to achieve this goal. If coupled with $^1ET/ET^b$ discrimination in the electronic coupling term, $^1ET/ET^b$ ratios comparable to those found in the photosynthetic reaction center could be achieved in synthetic photochemical energy storage systems.

REFERENCES AND NOTES

1. D. Holten *et al.*, *Biochim. Biophys. Acta* **592**, 461 (1980); N. W. Woodbury, M. Becker, D. Middendorf, W. W. Parson, *Biochemistry* **24**, 7516 (1985); J.-L. Martin, J. Breton, A. J. Hoff, A. Migus, A. Antonetti, *Proc. Natl. Acad. Sci. U.S.A.* **83**, 957 (1986); J. Breton, J.-L. Martin, A. Migus, A. Antonetti, A. Orszag, *ibid.*, p. 5121; M. R. Wasielewski and D. M. Tiede, *FEBS Lett.* **204**, 368 (1986); J. Breton, J.-L. Martin, J. Petrich, A. Migus, A. Antonetti, *ibid.* **209**, 37 (1986); C. Kirmaier and D. Holten, *Isr. J. Chem.* **28**, 79 (1988).
2. C. Kirmaier and D. Holten, *Photosynth. Res.* **13**, 225 (1987); G. Feher, J. P. Allen, M. Y. Okamura, D. C. Rees, *Nature* **339**, 111 (1989).
3. R. A. Marcus and N. Sutin, *Biochim. Biophys. Acta* **811**, 265 (1986).
4. D. Rehm and A. Weller, *Isr. J. Chem.* **8**, 259 (1970).
5. C. Creutz and N. Sutin, *J. Am. Chem. Soc.* **99**, 241 (1977).
6. J. L. Marshall, S. R. Stobart, H. B. Gray, *ibid.* **106**, 3027 (1984).
7. M. R. Wasielewski, M. P. Neimczyk, W. A. Sveck, E. B. Pewitt, *ibid.* **107**, 1080 (1985).
8. G. L. Closs, L. T. Calcaterra, N. J. Green, K. W. Penfield, J. R. Miller, *J. Phys. Chem.* **90**, 3673 (1986); G. L. Closs and J. R. Miller, *Science* **240**, 440 (1988).
9. M. R. Gunner, D. E. Robertson, P. L. Dutton, *J. Phys. Chem.* **90**, 3783 (1986); M. R. Gunner and P. L. Dutton, *J. Am. Chem. Soc.* **111**, 3400 (1989).
10. A. D. Joran *et al.*, *Nature* **327**, 508 (1987).
11. I. R. Gould, D. Ege, S. L. Mattes, S. Farid, *J. Am. Chem. Soc.* **109**, 3794 (1987).
12. L. S. Fox, thesis, California Institute of Technology, Pasadena (1989).
13. ———, J. L. Marshall, H. B. Gray, J. R. Winkler, *J. Am. Chem. Soc.* **109**, 6901 (1987).
14. For descriptions of the apparatus and techniques used in this study, see: J. R. Winkler, D. G. Nocera, T. L. Netzel, *J. Am. Chem. Soc.* **108**, 4451 (1986); J. R. Winkler, T. L. Netzel, C. Creutz, N. Sutin, *ibid.* **109**, 2381 (1987).
15. Standard error estimates are as follows: $\lambda = 1.06 \pm 0.03$ eV; $\ln(\nu_N\kappa_E) = 25.7 \pm 0.3$; $\nu_N\kappa_E = (1.5 \pm 0.5) \times 10^{11}$ s^{-1}; $H_{AB} = 24 \pm 4$ cm^{-1}.
16. R. A. Marcus, *Isr. J. Chem.* **28**, 205 (1988).
17. S. F. Rice and H. B. Gray, *J. Am. Chem. Soc.* **103**, 1593 (1981); *ibid.* **105**, 4571 (1983).
18. R. D. Brost, D. G. Harrison, D. O. K. Fjeldsted, S. R. Stobart, unpublished results.
19. B. S. Brunschwig, S. Ehrenson, N. Sutin, *J. Phys. Chem.* **90**, 3657 (1986).
20. The x-ray crystal structure of the Ir_2 complex with $A^+ = py^+$ served as a model for the λ_{OUT} calculation (*12*). The minimum volume sphere that encloses all nonhydrogen atoms of this structure, including van der Waals radii, has a diameter of 19.14 Å. Charge was assumed to transfer 8.30 Å from the midpoint of the Ir-Ir vector (3.05 Å from the center of the sphere) to the center of the py^+ ring (8.19 Å from the center).
21. The ground- and excited-state wave functions for H_2^+ and H_2 are simple examples; see C. A. Coulson, *Valence* (Oxford Univ. Press, London, 1961).
22. D. N. Beratan and J. J. Hopfield, *J. Am. Chem. Soc.* **106**, 1584 (1984); D. N. Beratan, J. N. Onuchic, J. J. Hopfield, *J. Chem. Phys.* **83**, 5325 (1985); D. N. Beratan, *J. Am. Chem. Soc.* **108**, 4321 (1986).
23. T. Kakitani and N. Mataga, *J. Phys. Chem.* **91**, 6277 (1987).
24. The ^1ET, ^3ET, and ET^b reactions are charge-shift processes, and the variations in λ_{OUT} are likely to be small (*23*). Since λ_{OUT} dominates the nuclear reorganization energy, it is reasonable that λ should not vary greatly among the three types of reactions. Under these circumstances, fluctuations in κ_E would yield vertically displaced parabolas for the different reactions. The fact that the data are well described by a single parabola suggests that variations in κ_E must also be small.
25. J. V. Caspar and T. J. Meyer, *J. Am. Chem. Soc.* **105**, 5583 (1983).
26. We thank B. S. Brunschwig for assistance with the λ_{OUT} calculation. The work of L.S.F. was supported by a graduate research fellowship from British Petroleum America. Research at the California Institute of Technology was supported by National Science Foundation grant CHE84-19828 (contribution 7977 from the Arthur Amos Noyes Laboratory). Research at Brookhaven National Laboratory was carried out under contract DE-AC02-76CH00016 with the U.S. Department of Energy and supported by its Division of Chemical Sciences, Office of Basic Energy Sciences.

7 September 1989; accepted 4 December 1989

Direct Coupling of Marine Invertebrate Spawning with Phytoplankton Blooms

MICHEL STARR, JOHN H. HIMMELMAN, JEAN-CLAUDE THERRIAULT

Spawning of green sea urchins and blue mussels may be triggered by a heat-stable metabolite released by various species of phytoplankton. Mussels require a higher phytoplankton density for a maximum response than urchins, perhaps because mussels are exposed to higher concentrations of phytoplankton as a result of their filtering activity. Phytoplankton as a spawning cue appears to integrate numerous physical and biotic factors indicating favorable conditions for larval growth and survival. Evolution of similar direct coupling of the larval phase with phytoplankton blooms may be common among marine invertebrates.

FOR HALF A CENTURY BIOLOGISTS have observed the close timing between the production of pelagic larvae by benthic invertebrates and phytoplankton blooms (*1*). This synchrony provides the obvious advantage of ensuring an abundant food supply for the larvae. However, the mechanisms accounting for this coupling are poorly understood. Most workers favor the hypothesis that gamete and larval release are controlled by physical environmental variables such as changes in temperature, salinity, photoperiod, and turbulence. However, only a few studies have shown a relation with a particular factor that could be confirmed in the laboratory (*2*).

An alternative hypothesis is that phytoplankton induces spawning. This possibility, although briefly discussed many years ago by Thorson (*1*), has received little attention. Himmelman (*3*) showed that spawning of the urchin, *Strongylocentrotus droebachiensis*, and of two species of chitons is synchronous with the spring phytoplankton outburst and that natural plankton collected with a 50-μm mesh net stimulates spawning in the laboratory. Subsequently, it was noted in mariculture work that high concentrations of phytoplankton induce spawning in *Mytilus californianus* (*4*). An analogous situation exists for species such as barnacles, which brood their embryos and later release pelagic larvae when food becomes abundant (*5*).

We examined the mechanisms that couple spawning of invertebrates and the spring blooming of phytoplankton (*6*). We tested the following hypotheses: (i) that phytoplankton stimulates spawning, (ii) that spawning can be caused by numerous species of phytoplankton, (iii) that phytoplankton at concentrations found in nature can stimulate spawning, and (iv) that spawning results from direct contact with phytoplankton cells (either chemical or nutritional) or from the detection of substances released by them.

The spawning experiments were performed with green sea urchins (*Strongylocentrotus droebachiensis*, 35 to 45 mm in diameter) and blue mussels (*Mytilus edulis*, 35 to 45 mm in length) collected in the St. Lawrence estuary shortly before natural spawning. They were kept in holding tanks, supplied with recirculated seawater containing no phytoplankton, at a temperature of 5° to 7°C and a salinity of 21 to 27 parts per mil.

M. Starr and J. H. Himmelman, GIROQ (Groupe Interuniversitaire de Recherche Océanographique du Québec) and Département de Biologie, Université Laval, Québec, Canada G1K 7P4.
J.-C. Therriault, Institut Maurice-Lamontagne, Ministère des Pêches et des Océans, C.P. 1000, Mont-Joli, Québec, Canada G5H 3Z4.